AD-Vol. 24
AMD-Vol. 123

SMART STRUCTURES AND MATERIALS

presented at
THE WINTER ANNUAL MEETING OF
THE AMERICAN SOCIETY OF MECHANICAL ENGINEERS
ATLANTA, GEORGIA
DECEMBER 1–6, 1991

sponsored by
THE AEROSPACE DIVISION AND
THE APPLIED MECHANICS DIVISION, ASME

coordinating editor
GEORGE K. HARITOS
AFSOR/CC, BOLLING AFB

contributing editor
A. V. SRINIVASAN
UNITED TECHNOLOGIES

THE AMERICAN SOCIETY OF MECHANICAL ENGINEERS
345 East 47th Street □ United Engineering Center □ New York, N.Y. 10017

AD-Vol. 24/AMD-Vol. 123, Smart Structures and Materials
ASME 1991

MECHANICS CONCEPTS FOR FAILURE IN FERROELECTRIC CERAMICS

Z. Suo
Department of Mechanical Engineering
University of California
Santa Barbara, California

Abstract

The article reviews mechanics concepts suitable for analyzing defects (cracks, domain walls, etc.) in ferroelectric ceramics. Constitutive laws are summarized for dielectric, electrostrictive and piezoelectric ceramics. The formulation is based on an energy function of strain and induction, and a few experimental facts. Also summarized are the differential equations that govern stress and electric fields. Griffith's energy release rate is examined for a body containing a defect under applied force and voltage, followed by applications to multilayer capacitors, conducting cracks, impermeable cracks and domain bands. A generalized Irwin-Kies relation is presented, explaining the peculiar results that the energy release rates are negative for non-conducting cracks but positive for conducting cracks. Singular fields around impermeable and conducting cracks are contrasted. The possibility of using the energy release rate to correlate breakdown resistance of a ceramic is considered.

1. Introduction

I shall review the basic concepts and some current work on deformation and degredation of ferroelectric ceramics; several papers by the colleagues at UCSB on the subject are listed at the end of the article. There has recently been a considerable resurgence in the basic study of ferroelectric ceramics, due to their great potentials, as well as the reliability uncertainties in applications.

Ferroelectric ceramics have great potential for applications — capacitors, sensors, actuators and memories — to name a few. However, various degradation mechanisms stand in the way for wider applications. Ferroelectric ceramics are brittle and susceptible to cracking; one remedy is to embed them into polymer matrices. Reliability problems associated with regular composites are of concern. Dielectric breakdown sets a limit to the applied field, which in turn limits the attainable actuation strain. Polarization switch could be used for non-volatile memories, but the hysteresis loop vanishes after 10^{12} cycles even for thin films.

The work reported here represents our initial effort to address these issues. The field now is polarized in two extremes: the experimental observations that are not correlated, and the theoretical speculations that are not validated. The understanding will be improved in the future, should we coordinate our efforts in processing, testing and modeling of these materials.

2. Constitutive Laws

Subject a ceramic slab to a uniform electric field (Fig. 1). Two quantities are measured independently: the voltage V and the charge Q. The electric field E and the electric induction D (i.e., the electric displacement) are defined by

$$E = V / h, \quad D = Q / S, \tag{2.1}$$

where h is the height of the ceramic and S the area covered by one electrode. The recorded Q-V curve is scaled to a D-E curve according to (2.1). The latter characterizes the dielectric property of a material.

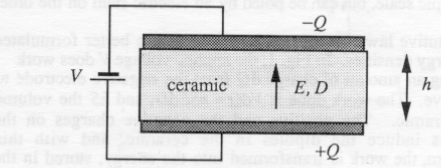

Fig. 1 A ceramic loaded with V.

Figure 2 sketches three types of behaviors. A *dielectric* such as an alumina is linear:

$$D = \varepsilon E. \tag{2.2}$$

The proportionality constant defines the permittivity. For a typical ceramic, $\varepsilon \sim 10^{-10}$ F/m, ten times the value of the vacuum. The permittivity results from atomic dipole stretching by the electric field.

In *relaxors*, such as $Pb(Mg_{1/3}Nb_{2/3})O_3$ (PMN) and various compositions of PMN:$PbTiO_3$, the dipoles are stretched to a much larger extent . These materials are nonlinear, and the D-E curve can be fitted by an odd function, e.g.,

$$E = \beta D + \beta' D^3 + \ldots \tag{2.3}$$

The motion of the atoms is constrained after being stretched to a certain extent, leading to the saturation on the D-E curve. The tangential permittivity of a relaxor can vary with E by two orders of magnitude, around 10^{-7} F/m.

A *ferroelectric* crystal has a spontaneous polarization, P_s; the

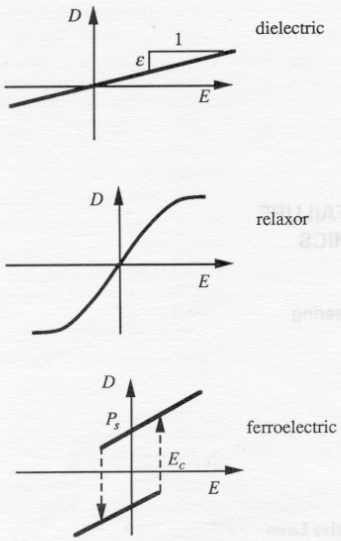

Fig. 2 *D-E* relation for a few materials.

polar direction can be switched by a suitable electric field, E_c. An idealized hysteresis loop is drawn in Fig. 2, jumping between two linear branches:

$$D = \pm P_s + \varepsilon E. \tag{2.4}$$

For a $BaTiO_3$ crystal, $P_s \sim 0.26$ C/m^2 and $\varepsilon \sim 10^{-8}$ F/m. A ferroelectric ceramic is not spontaneously polarized at the macroscopic scale, but can be poled by an electric field on the order 1 MV/m.

Constitutive laws for reversible materials are better formulated using energy densities. In Fig. 1, the applied voltage V does work by moving an amount of charge dQ from the negative electrode to the positive. The work done is $VdQ = hSEdD$, and hS the volume of the ceramic. The positive and the negative charges on the electrodes induce the dipoles in the ceramic, and with this mechanism, the work is transformed into the energy, stored in the ceramic. The energy in the ceramic can also be increased by stress. Consequently, the energy per unit volume varies as

$$du = EdD + \sigma d\gamma, \tag{2.5}$$

where γ is the strain and σ the stress. The energy density is a function of induction and strain, assuming the temperature is held constant during the loading. Given $u(D, \gamma)$, the constitutive laws are derived from

$$E = (\partial u / \partial D)_\gamma, \quad \sigma = (\partial u / \partial \gamma)_D. \tag{2.6}$$

In the remaining of the section, the procedure is illustrated by one-dimensional responses, followed by an extension to the multiaxial state.

A regular dielectric is characterized by a quadratic:

$$u = \frac{1}{2}\beta D^2 + \frac{1}{2}c\gamma^2, \tag{2.7}$$

where β is the inverse of the permittivity, and c is the stiffness. Taking the derivatives, one obtains the constitutive relations

$$E = \beta D, \quad \sigma = c\gamma. \tag{2.8}$$

The dielectric and elastic responses are assumed to be decoupled in the above. In reality, an electric field stretches dipoles, causing both induction and strain. The strain induced by the electric field is referred to as electrostrictive strain. It is a small effect for regular dielectrics and hence ignored.

Relaxors have large electrostrictive strains and nonlinear *D-E* relations, but hysteresis is small enough to be neglected in most defect analysis. Two additional experimental facts simplify the matter: i) γ is linear in σ when $D = 0$ and, ii) γ is quadratic in D when $\sigma = 0$. To incorporate these, it is convenient to use another energy defined as

$$g = u - \gamma\sigma. \tag{2.9}$$

Comparing with (2.5), one obtains

$$dg = EdD - \gamma d\sigma. \tag{2.10}$$

Once $g(D, \sigma)$ is prescribed, the constitutive relations are derived from

$$E = (\partial g / \partial D)_\sigma, \quad \gamma = -(\partial g / \partial \sigma)_D \tag{2.11}$$

Consistent with the two experimental facts, the energy function for relaxors is

$$g(D,\sigma) = -\frac{1}{2}s\sigma^2 - Q\sigma D^2 + \int f(D)dD, \tag{2.12}$$

where s is the compliance, Q the electrostriction constant, and $f(D)$ is an odd function of form (2.3). Taking the derivatives, one obtains the constitutive relations

$$\gamma = s\sigma + QD^2, \quad E = -2Q\sigma D + f(D). \tag{2.13}$$

When $f(D) = D/\varepsilon$, (2.13) describes a regular dielectric, for which γ is also quadratic in E when $\sigma = 0$ — that is, $\gamma = Q\varepsilon^2 E^2$. However, γ is not quadratic in E for relaxors with nonlinear f.

It is difficult to formulate a complete constitutive law for ferroelectrics; the energy function that reflects the hysteresis is complicated. However, for many applications an expression for a linearized branch is sufficient:

$$u(D,\gamma) = \frac{1}{2}\beta D^2 + \frac{1}{2}c\gamma^2 + hD\gamma, \tag{2.14}$$

where h is the piezoelectric constant. For PZT, $\beta \sim 10^8$ m/F, $c \sim 10^{11}$ N/m^2, $h \sim 10^{10}$ V/m. The constitutive relations are

$$E = \beta D + h\gamma, \quad \sigma = c\gamma + hD. \tag{2.15}$$

Both D and γ are measured from the spontaneous state. A spontaneous polarization and a residual strain must be included in solving some problems.

The above can be generalized to multiaxial material responses. The results for isotropic relaxors are given explicitly below. The electrostrictive constants constitute a fourth-rank tensor with the same symmetry as the elasticity tensor. When polarized along the x-axis, in either positive or negative direction, a relaxor elongates in x and shrinks in y. The two electrostriction constants are defined by

$$\gamma_{xx} = Q_{1111}D_x^2, \quad \gamma_{yy} = Q_{2211}D_x^2. \tag{2.16}$$

For PMN, $Q_{1111} = 0.019$ m^4/C^2 and $Q_{2211} = -0.006$ m^4/C^2.

In tensor notation one writes

$$\gamma_{ij} = \frac{1}{2\mu}\left(\sigma_{ij} - \frac{\nu}{1+\nu}\sigma_{kk}\delta_{ij}\right) + (Q_{1111} - Q_{1122})D_iD_j + Q_{1122}D_kD_k\delta_{ij}. \tag{2.17}$$

The elasticity is also included, where μ is the shear modulus and ν the Poisson's ratio. The electric field is given by

$$E_i = -2(Q_{1111} - Q_{1122})\sigma_{ij}D_j - 2Q_{1122}\sigma_{kk}D_i + D_i f(D)/D, \tag{2.18}$$

where $D = (D_iD_i)^{1/2}$, and f can be determined by applying the field in any direction. The corresponding energy density is

$$g(\sigma, \boldsymbol{D}) = -\frac{1}{4\mu}\left(\sigma_{ij}\sigma_{ij} - \frac{\nu}{1+\nu}\sigma_{kk}\sigma_{ll}\right) - (Q_{1111} - Q_{1122})\sigma_{ij}D_iD_j - Q_{1122}\sigma_{ll}D_kD_k + \int_0^D f(D)dD. \tag{2.19}$$

As one can see, the complete constitutive law for a relaxor only requires a few measurements.

3. Differential Equations

In analyzing the nonlinear field around a defect, in addition to the constitutive laws, the differential equations in elasticity and electrostatics are called for. They are collected below.

Subject a ceramic to a field of displacement $\boldsymbol{u}$ and electric potential ϕ. The strain γ and the electric field $\boldsymbol{E}$ are derived from gradients:

$$\gamma_{ij} = \frac{1}{2}\left(u_{i,j} + u_{j,i}\right), \quad E_i = -\phi_{,i}. \tag{3.1}$$

Define the stress σ and the induction $\boldsymbol{D}$ as work-conjugates, respectively, to γ and $\boldsymbol{E}$. The principle of virtual work is postulated — that is, for any compatible virtual change, the energy inside the material equals the applied work:

$$\int\left(\sigma_{ij}\delta\gamma_{ji} + E_i\delta D_i\right)dv = \int\left(t_j\delta u_j + \phi\delta\omega\right)ds, \tag{3.2}$$

where $\boldsymbol{t}$ is the force and ω the charge, per unit area, externally supplied on the interface. The body force and extrinsic bulk charge are taken to be negligible.

Equations (3.1) and (3.2) imply, as can be verified using the divergence theorem, that σ and $\boldsymbol{D}$ are divergence free:

$$\sigma_{ij,i} = 0, \quad D_{i,i} = 0, \tag{3.3}$$

and that across an interface, they jump by

$$n_i\left[\sigma_{ij}^{+} - \sigma_{ij}^{-}\right] = t_j, \quad n_i\left[D_i^{+} - D_i^{-}\right] = -\omega, \tag{3.4}$$

where $\boldsymbol{n}$ is the unit normal to the interface pointing from the + side.

4. Energy Release Rate

4.1 Definition

Griffith's energy accounting defines the driving force for defects. Load a test-piece, which contains a defect (crack, domain wall, etc.), by a displacement Δ and a charge Q. Denote the work-conjugate force as F, and voltage V. The total energy in the test-piece, U, varies as

$$\mathrm{d}U = F\mathrm{d}\Delta + V\mathrm{d}Q - \mathcal{G}\mathrm{d}A, \tag{4.1}$$

where A is the area of the defect. The principle of vertual work is recovered when A remains fixed during the loading. For a given test-piece, the function $U(\Delta, Q, A)$ can be computed by analyzing the stress and electric fields. Consequently, (4.1) defines $\mathcal{G}$ as the driving force for the defect area A:

$$\mathcal{G} = -\left(\partial U / \partial A\right)_{\Delta,Q}. \tag{4.2}$$

Test-pieces are usually loaded by F and V. A more convenient, but equivalent, energy is defined by

$$\Pi = U - F\Delta - VQ. \tag{4.3}$$

For historical reasons, Π is referred to as potential energy. A comparison with (4.1) gives

$$\mathrm{d}\Pi = -\Delta\mathrm{d}F - Q\mathrm{d}V - \mathcal{G}\mathrm{d}A. \tag{4.4}$$

Once the potential energy, $\Pi(F, V, A)$, is calculated for a test-piece, $\mathcal{G}$ is obtained by

$$\mathcal{G} = -\left(\partial\Pi / \partial A\right)_{F,V}. \tag{4.5}$$

The definition is rather abstract; a few applications will clarify the meaning of $\mathcal{G}$.

4.2 Applications

Consider a capacitor made of two metal plates with an air gap. A metal foil is half way inserted into the capacitor and held at voltage V with respect to the two electrodes (Fig. 3). An attractive coulomb force draws the foil into the gap. Let us compute the force on the unit width of the foil, denoted as $\mathcal{G}$. Denote Q as the charge on the foil per unit width, l the insertion length, and ε and permittivity of the air. The energy per unit width of the system is $U = VQ/2$, or, $\Pi = U - VQ = -VQ/2$. The right-hand part of the capacitor is absent of the field, and the left is a two-layer capacitor with $Q = 4\varepsilon Vl / h$. One expresses the energy as $\Pi(V,l) = -2\varepsilon V^2 l / h$. Differentiate Π with respect to l holding V constant, and one obtains

$$\mathcal{G} = 2\varepsilon V^2 / h. \tag{4.6}$$

The interpretation is clear: $\mathcal{G}$ is the coulomb force on unit width of the foil, sucking it into the capacitor.

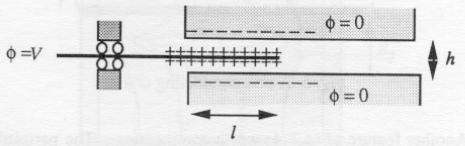

Fig. 3 A metal foil is drawn into a capacitor.

Now if the capacitor is made of a ceramic instead of the air, the electrostatic field still tends to attract the metal foil into the capacitor. Of necessity, the ceramic also sustains a distributed force, intensified around the tip of the foil. This situation occurs in multilayer capacitors, where fracture has been observed to initiate from the tip of embedded electrodes. The detailed mechanisms of fracture are unclear now. Nonetheless, for a virtual extension of the foil, the energy of the system decreases by $\mathcal{G}$, still given by (4.6).

Depicted in Fig. 4 is a conducting crack held at voltage V with respect to the electrodes. For the crack to extend a unit distance, the energy of the system decreases by $\mathcal{G}$ as given by (4.6). This energy must be spent on breaking the atomic bonds and any other processes associated with cracking. One such process in ferroelectrics is dipole switching at the crack tip. No mechanistic description of this energy transfer is now available. However, it is possible to correlate fracture on the basis of $\mathcal{G}$, as will be discussed in a later section.

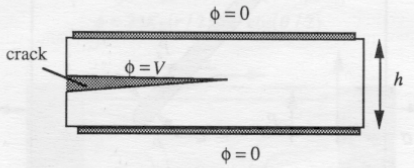

Fig. 4 A conducting crack.

Figure 5 illustrates a ceramic with a non-conducting notch of thickness δ. The permittivities of the ceramic and the medium inside the notch (say, the air) are, respectively, ε and ε_c. Computed with the same procedure, the energy release rate is

$$\mathcal{G} = -\frac{\varepsilon V^2}{2h}\left[\frac{\left(\varepsilon / \varepsilon_c - 1\right)\left(\delta / h\right)}{1 + \left(\varepsilon / \varepsilon_c - 1\right)\left(\delta / h\right)}\right]. \tag{4.7}$$

Most prominently, this energy release rate is negative, since the permittivity is larger in the ceramic than in the air. This fact has prompted the conjecture that a non-conducting crack will never grow under electrical filed. Inadequate mechanistic description of the fracture process prevents a definite discussion here, but one should

not jump into the conclusion without performing experiments. The intensified electric field at the crack tip can cause many irreversible processes, which are not captured by $\mathcal{G}$ based on the reversible field. It is likely that the ferroelectric hysteresis at the crack tip would cause slow crack growth under alternating field.

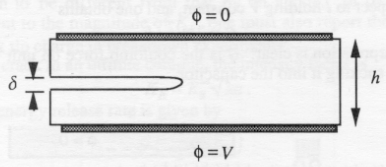

Fig. 5 A non-conducting crack.

Another feature of (4.7) is worth commenting. The permittivity of a ferroelectric is over 10^3 times that of the air. An assertion is that the crack is impermeable — that is, $D_n = 0$ holds on crack faces. The assertion simplifies the mathematical analysis significantly for some problems. For the present problem, this simplification yields

$$\mathcal{G} = -\varepsilon V^2 / 2h. \tag{4.8}$$

Compared with (4.7), the impermeable crack assumption *overestimates* the magnitude of $\mathcal{G}$; it becomes accurate only when

$$(\varepsilon / \varepsilon_c)(\delta / h) \gg 1. \tag{4.9}$$

Conditions of this sort have been identified for other crack configurations by McMeeking (1989).

At the room temperature, a $BaTiO_3$ crystal is tetragonal, with about 1% difference in the a and c lattice constants, and with a spontaneous polarization along the c-axis. Axes a and c can be switched, along with the polar axis, by electric field and stress. Two domains with perpendicular polar axes are usually separated by a domain wall at 45° from the axes, so that no polarization charge resides on the domain wall.

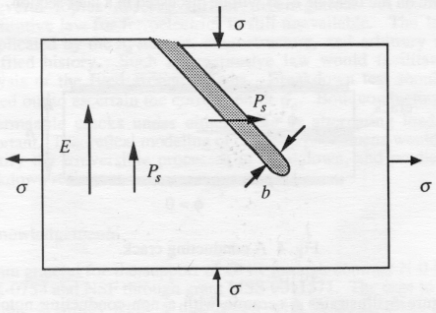

Fig. 6 a-domain band in an infinite c-domain.

Domain switching can degrade ferroelectrics. When an electric field is applied to a ferroelectric, stress is induced by the actuation force, or by mismatch among domains and grains. The following shows that the stress can switch domains.

Figure 6 illustrates a band of a-domain, of thickness on the order microns, advancing in an infinite c-domain. An electric field is applied along the c-axis, and remote stresses are applied equivalent to a pure shear on the band. The hydrostatic stress does not switch dipoles and hence ignored. The electric field tends to retard banding but the stress facilitate. The energy release rate for banding is (He *et al*. 1991)

$$\mathcal{G} = 2\gamma_s \sigma b - P_s E b \tag{4.10}$$

where $\gamma_s = (c - a)/a$ is the strain involved in the a-to-c transition, P_s the spontaneous polarization, and b the band thickness.

Additional domain walls form as the band grows, with surface energy Γ. Since the a-to-c transition involves only a shuffling of atoms within the unit cell, it is reasonable to expect the process dissipates little energy. Consequently, the energy decrease, $\mathcal{G}$, should be spent on creating the walls, namely, the band advances if

$$\mathcal{G} = 2\Gamma. \tag{4.11}$$

Although one does not know the mechanistic details in this energy transfer, the mere anticipation of reversibility allows one to estimate, using the basic crystal properties, the stress and field needed for banding. For $BaTiO_3$ under $E = 0.5$ MV/m, a shear stress $\sigma \sim 10$ MPa is sufficient to cause a band of thickness $b = 1$ μm (He *et al*. 1991).

4.3 Irwin-Kies Relation

To better understand the result concerning the negative energy release rate for impermeable cracks, I shall present a generalized Irwin-Kies relation, which holds for linear piezoelectrics. Load a linear piezoelectric test-piece by voltage V and force F, and the potential energy is a quadratic

$$\Pi(V, F, A) = -\frac{1}{2} C_e V^2 - \frac{1}{2} C_m F^2 - C_p V F, \tag{4.12}$$

where C_e is the electrical capacitance, C_m the mechanical compliance, and C_p the piezoelectric compliance; they depend on crack area A. Their meanings are immediately clear:

$$\begin{aligned} Q &= -(\partial \Pi / \partial V)_{A,F} = C_e V + C_p F, \\ \Delta &= -(\partial \Pi / \partial F)_{A,V} = C_m F + C_p V \end{aligned} \tag{4.13}$$

The energy release rate is given by

$$\mathcal{G} = -\left(\frac{\partial \Pi}{\partial A}\right)_{V,F} = \frac{V^2}{2}\frac{dC_e}{dA} + \frac{F^2}{2}\frac{dC_m}{dA} + FV\frac{dC_p}{dA} \tag{4.14}$$

The special case involving only the force is called Irwin-Kies relation in the fracture mechanics.

Now one can explain the sign of $\mathcal{G}$ in terms of familiar concepts. Consider the case when $F = 0$, so that only the electrical term is left in (4.14). It is known that the capacitance of a system decreases if a lower permittivity medium is incorporated, but increases if a higher permittivity or a conducting medium is incorporated. Thus,

$$dC_e/dA < 0, \quad \text{for impermeable cracks,} \tag{4.15}$$

and

$$dC_e/dA > 0, \quad \text{for conducting cracks.} \tag{4.16}$$

Comparing with (4.14), one obtains the correct signs for $\mathcal{G}$.

5. Breakdown Resistance

The definition of $\mathcal{G}$ applies to both linear and nonlinear materials. Of particular concern here are dielectrics, relaxors and ferroelectrics. Owing to the great success of using $\mathcal{G}$ to correlate fracture resistance under mechanical loading, a natural question is whether $\mathcal{G}$ can be used to correlate the breakdown resistance under electrical loading.

Traditionally, breakdown strength of a dielectric is determined by loading a test-piece of a standard shape. The results (say, the critical voltage) obtained this way depend on the particular test-piece used. However, if a notched test-piece is used, the critical energy release rate, $\mathcal{G}_c$, could be independent of the shape and size of the test-piece. In this sense, $\mathcal{G}_c$ should be a better measure of breakdown

strength.

Breakdown is a complicated phenomenon; the proposition of using one parameter, $\mathcal{G}_c$, to correlate the breakdown strength of a ceramic determined by different test-pieces requires some explanations. One premise is that the breakdown is indeed caused by cracks, as introduced, say, in ceramic processing. A second premise is that a mechanism must exist which transfers the electrical energy to break atomic bonds ahead of the crack tip, or any other processes identified with the breakdown. A third premise is that the electric field in the overall test-piece, at the breakdown, is low enough so that the material is still described by the standard constitutive laws. The third corresponds to the small-scale yielding concept in the fracture mechanics.

Very little, experimental or theoretical, is known to ascertain these. However, the validity of the correlation can be directly verified by measuring $\mathcal{G}_c$ for various shapes of test-pieces.

There is no reason to expect that $\mathcal{G}_c$ determined under electrical loading should be the same as the fracture resistance determined under mechanical loading. For the two types of failure can be accompanied by different irreversible processes.

6. Crack Tip Field

Crack tip field in piezoelectrics has been analyzed, both impermeable (Suo *et al.* 1991) and conducting cracks (Suo 1991). In this presentation, I will focus on non-piezoelectric ceramics. An example is unpoled ferroelectrics; the polycrystalline, multi-domain structure cancels the macroscopic piezoelectricity. The ceramics have linear *D-E* relations with large permittivities.

6.1 Impermeable Crack

Figure 7 shows an impermeable crack — that is, $D_y = 0$ holds on the crack faces. The remotely applied field E_y^∞ is diverted around the crack to satisfy the boundary condition. However, the crack does not perturb E_x^∞, which is excluded from Fig. 7. Let (r, θ) be the polar coordinates centered at the crack tip on the right. The electric field is square root singular in r as the crack tip is approached. The intensity factor, K_{IV}, is defined such that at a distance r ahead of the crack tip

$$D_y = K_{IV}(2\pi r)^{-1/2}. \tag{6.1}$$

The crack tip field, to the leading order, is

$$D_x = -K_{IV}(2\pi r)^{-1/2}\sin(\theta/2), \tag{6.2a}$$

$$D_y = K_{IV}(2\pi r)^{-1/2}\cos(\theta/2), \tag{6.2a}$$

$$\phi = -\frac{2}{\varepsilon}K_{IV}(r/2\pi)^{1/2}\sin(\theta/2). \tag{6.2c}$$

The intensity factor, K_{IV}, reflects the magnitude of the applied load transferred to the crack tip. The form of the singular field is independent of the test-piece. In the fracture mechanics, the existence of such a universal field is used to explain the one-parameter correlation.

The energy release rate is connected with the intensity factor as

$$\mathcal{G} = -\frac{1}{2\varepsilon}K_{IV}^2, \tag{6.3}$$

Note that $\mathcal{G}$ is always negative for the impermeable crack, consistent with the previous results. For isotropic materials, a closer examination of Fig. 7 reveals that the nature of the crack tip field is unchanged if the direction of E_y^∞ is reversed. Consequently, the sign of K_{IV} has no effect on breakdown, and $\mathcal{G}$ and K_{IV} are equivalent in characterizing the applied load.

Since the differential equations are similar for a crack under either electric field or anti-plane shear stress, solutions for many geometries can be found in handbooks of stress intensity factors. For example, for the crack in an infinite ceramic in Fig. 7, one finds

$$K_{IV} = \varepsilon E_y^\infty \sqrt{\pi a}, \tag{6.4}$$

where $2a$ is the crack length. The energy release rate is therefore

$$\mathcal{G} = -\frac{\pi}{2}\varepsilon a\left(E_y^\infty\right)^2 \tag{6.5}$$

For a $BaTiO_3$ ceramic with $\varepsilon = 1.6\times 10^{-8}$ F/m under $E_y^\infty = 1$ MV/m, a defect of size $a = 10^{-4}$ m sustains $\mathcal{G} = -2.5$ J/m^2.

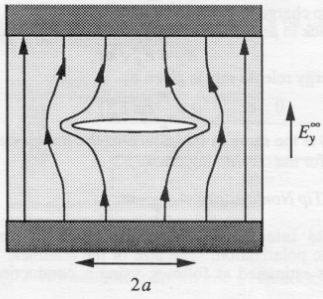

Fig. 7 An impermeable crack.

6.2 Conducting Crack

A crack becomes conducting if it enclaves electrolytes or its surfaces are diffusive of ions. The boundary condition is that $E_x = 0$ on the crack faces. In contrast to an impermeable crack, a conducting crack does not intensify the electric field perpendicular to the crack, but does intensify the parallel field to conform to the boundary condition. The singular field takes a different form from that of the impermeable cracks, but is still square root singular. A different intensity factor, K_E, is defined by the electric field direct ahead of the crack

$$E_x = K_E(2\pi r)^{-1/2}. \tag{6.6}$$

The crack tip field is given by

$$E_x = K_E(2\pi r)^{-1/2}\cos(\theta/2), \tag{6.7a}$$

$$E_y = K_E(2\pi r)^{-1/2}\sin(\theta/2), \tag{6.7a}$$

$$\phi = 2K_E(r/2\pi)^{1/2}\cos(\theta/2). \tag{6.7c}$$

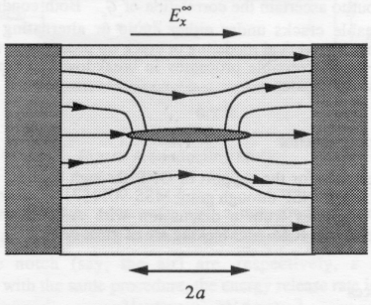

Fig. 8 A conducting crack.

The energy release rate is related to the intensity factor via

$$\mathcal{G} = \frac{1}{2}\varepsilon K_E^2. \tag{6.8}$$

Unlike impermeable cracks, the energy release rate is positive for conducting cracks. Another difference can be appreciated by

examining Fig. 8. The sign of K_E does make a difference on the crack tip field. With the present sign convention, $K_E > 0$ corresponds to the tip with the positive charge (the tip on the right in Fig. 8), and $K_E < 0$ the tip with the negative charge (the tip on the left in Fig. 8). This difference is likely to affect breakdown. For example, the breakdown of a dielectric liquid induced by a cathode is known to be different from that by an anode. In (6.8), $\mathcal{G}$ is equivalent to the magnitude of K_E; one must also report the sign of the crack tip charge in breakdown experiments.

For a crack in an infinite ceramic, the intensity factor is

$$K_E = E_x^{\infty}\sqrt{\pi a}, \tag{6.9}$$

and the energy release rate is given by

$$\mathcal{G} = \frac{\pi}{2}\varepsilon a\left(E_x^{\infty}\right)^2. \tag{6.10}$$

Note that $\mathcal{G}$ is the same in magnitude as the impermeable crack, but is positive for the conducting crack.

6.3 Crack Tip Nonlinearity

The field intensified around the crack tip can switch the ferroelectric polarization. The size of the nonlinear zone around a crack tip is estimated as follows, using a conducting crack as an example.

Assume the nonlinearity becomes significant when $E = E_c$. Using (6.5) one obtains the size of the nonlinear zone

$$r_c = \frac{1}{2\pi}\left(K_E / E_c\right)^2. \tag{6.11}$$

For an isolated crack of length $2a$ under remote loading E_x^{∞}, the intensity factor is given by (6.9), so that

$$r_c / a = \frac{1}{2}\left(E_x^{\infty} / E_c\right)^2. \tag{6.12}$$

Thus, the nonlinear zone is a fraction of the crack size so long as the remote load is below the critical field.

The energy release rate in (6.10), calculated by ignoring the nonlinearity, is anticipated to be accurate when r_c/a is small.

7. Concluding Remarks

Several topics deserve further investigation. A complete constitutive law for ferroelectrics is still unavailable. The law is complicated by the hysteresis, microstructure, and arbitrary stress and filed history. Such a constitutive law would facilitate the analysis of the filed around defects. Breakdown test should be carried out to ascertain the correlation of $\mathcal{G}_c$. Both conducting and impermeable cracks under either static or alternating loads are important. Theoretical modeling of crack tip phenomena would help identify the irreversible processes in breakdown, and predict the breakdown resistance.

Acknowledgements

I am grateful for the support of ONR through contract N-0-0014-86-K-0753 and NSF through grant MSS-9011571. The urge to write Section 4 comes from a discussion with A.G. Evans. Many discussions with R.M. McMeeking are of great help.

References

He, M.-Y., Suo, Z., McMeeking, R.M. and Evans, A.G., 1991, "Mechanics of Some Degradation Mechanisms in Ferroelectric Actuators," submitted for publication.

McMeeking, R.M., 1987, "On Mechanical Stresses at Cracks in Dielectrics with Application to Dielectric Breakdown," *J. Appl. Phys.* **62**, 3116-3122.

McMeeking, R.M., 1989, "Electrostrictive Stress near Crack-like Flaws," *J. Appl. Math. Phys.* **40**, 615-627.

McMeeking, R.M., 1990, "A J-Integral for the Analysis of Electrically Induced Mechanical Stress at Cracks in Elastic Dielectrics," *Int. J. Eng. Sci.* **28**, 605-613.

Suo, Z., 1991, "Conducting Cracks in Piezoelectrics," submitted for publication.

Suo, Z., Kuo, C.-M., Barnett, D.M. and Willis, J.R., 1991, "Fracture Mechanics for Piezoelectric Ceramics," *J. Mech. Phys. Solids*. (in press).